

# Measurement of the $K_L$ meson lifetime with the KLOE detector

The KLOE Collaboration

F. Ambrosino<sup>d</sup>, A. Antonelli<sup>a</sup>, M. Antonelli<sup>a</sup>, C. Bacci<sup>i</sup>,  
 P. Beltrame<sup>a</sup>, G. Bencivenni<sup>a</sup>, S. Bertolucci<sup>a</sup>, C. Bini<sup>g</sup>,  
 C. Boisse<sup>a</sup>, V. Bocci<sup>g</sup>, F. Bossi<sup>a</sup>, D. Bowering<sup>a,k</sup>, P. Branchini<sup>i</sup>,  
 R. Calbi<sup>g</sup>, P. Campana<sup>a</sup>, G. Capon<sup>a</sup>, T. Capussela<sup>d</sup>,  
 F. Ceradini<sup>i</sup>, S. Chi<sup>a</sup>, G. Chieffari<sup>d</sup>, P. Ciambrone<sup>a</sup>,  
 S. Conetti<sup>k</sup>, E. De Lucia<sup>g</sup>, A. De Santis<sup>g</sup>, P. De Simone<sup>a</sup>,  
 G. De Zorzi<sup>g</sup>, S. Dell'Agnello<sup>a</sup>, A. Denig<sup>b</sup>, A. Di Domenico<sup>g</sup>,  
 C. Di Donato<sup>d</sup>, S. Di Falco<sup>e</sup>, B. Di Micco<sup>i</sup>, A. Doria<sup>d</sup>,  
 M. Dreucci<sup>a</sup>, G. Felici<sup>a</sup>, A. Ferrari<sup>i</sup>, M. L. Ferrer<sup>a</sup>,  
 G. Finocchiaro<sup>a</sup>, C. Forti<sup>a</sup>, P. Franzini<sup>g</sup>, C. Gatti<sup>a</sup>, P. Gauzzi<sup>g</sup>,  
 S. Giovannella<sup>a</sup>, E. Gorini<sup>c</sup>, E. Graziani<sup>i</sup>, M. Incagli<sup>e</sup>,  
 W. Kluge<sup>b</sup>, V. Kulikov<sup>m</sup>, F. Lacava<sup>g</sup>, G. Lanfranchi<sup>a,l</sup>,  
 J. Lee-Franzini<sup>a,j</sup>, D. Leone<sup>g</sup>, M. Martini<sup>a</sup>, P. Massarotti<sup>d</sup>,  
 W. Mei<sup>a</sup>, S. Meola<sup>d</sup>, S. Miscetti<sup>a</sup>, M. Moulson<sup>a</sup>, S. Muller<sup>b</sup>,  
 F. Murtas<sup>a</sup>, M. Napolitano<sup>d</sup>, F. Nguyen<sup>i</sup>, M. Palutan<sup>a</sup>,  
 E. Pasqualucci<sup>g</sup>, A. Passeri<sup>i</sup>, V. Patera<sup>a,f</sup>, F. Perfetto<sup>d</sup>,  
 L. Pontecorvo<sup>g</sup>, M. Primavera<sup>c</sup>, P. Santangelo<sup>a</sup>, E. Santovetti<sup>h</sup>,  
 G. Saracino<sup>d</sup>, B. Sciascia<sup>a</sup>, A. Sciubba<sup>a,f</sup>, F. Scuri<sup>e</sup>, I. Sligoi<sup>a</sup>,  
 T. Spadaro<sup>a</sup>, M. Testa<sup>g</sup>, L. Tortora<sup>i</sup>, P. Valente<sup>a</sup>,  
 B. Valeriani<sup>b</sup>, G. Venanzoni<sup>e</sup>, S. Veneziano<sup>g</sup>, A. Ventura<sup>c</sup>,  
 R. Versaci<sup>i</sup>, G. Xu<sup>a,i</sup>

<sup>a</sup>Laboratori Nazionali di Frascati dell'INFN, Frascati, Italy.

<sup>b</sup>Institut für Experimentelle Kernphysik, Universität Karlsruhe, Germany.

<sup>c</sup>Dipartimento di Fisica dell'Università e Sezione INFN, Lecce, Italy.

<sup>d</sup>Dipartimento di Scienze Fisiche dell'Università "Federico II" e Sezione INFN, Napoli, Italy

<sup>e</sup>Dipartimento di Fisica dell'Università e Sezione INFN, Pisa, Italy.

<sup>f</sup>Dipartimento di Energetica dell'Università "La Sapienza", Roma, Italy.

<sup>g</sup>Dipartimento di Fisica dell'Università di Roma, "La Sapienza" e Sezione INFN,

Roma, Italy.

<sup>h</sup>Dipartimento di Fisica dell'Università di Roma 2, "Tor Vergata" e Sezione INFN, Roma, Italy.

<sup>i</sup>Dipartimento di Fisica dell'Università di Roma 3 e Sezione INFN, Roma, Italy.

<sup>j</sup>Physics Department, State University of New York at Stony Brook, USA.

<sup>k</sup>Physics Department, University of Virginia, USA.

<sup>l</sup>Permanent address: Institute of High Energy Physics, CAS, Beijing, China.

<sup>m</sup>Permanent address: Institute for Theoretical and Experimental Physics, Moscow, Russia.

<sup>n</sup>Permanent address: High Energy Physics Institute, Tbilisi State University, Tbilisi, Georgia.

<sup>1</sup> Corresponding author: Gaia Lanfranchi, INFN - LNF, CP 13, 00044 Frascati (Roma), Italy; e-mail: gaia.lanfranchi@lnf.infn.it

---

Abstract

We present a measurement of the  $K_L$  lifetime using the KLOE detector. From a sample of  $4 \cdot 10^8$   $K_S K_L$  pairs following the reaction  $e^+ e^- \rightarrow K_S K_L$  we select  $15 \cdot 10^6$   $K_L \rightarrow \pi^0 \pi^0 \pi^0$  decays tagged by  $K_S \rightarrow \pi^+ \pi^-$  events. From a fit of the proper time distribution we find  $\tau_L = (50.92 \pm 0.17_{\text{stat}} \pm 0.25_{\text{sys}})$  ns. This is the most precise measurement of the  $K_L$  lifetime performed up to date.

PACS:

keywords:

---

## 1 Introduction

The  $K_L$  lifetime is necessary to determine its semileptonic partial widths from the branching ratios (BR). The partial widths can be used to extract the CKM matrix element  $|V_{us}|$ . Present knowledge of  $\tau(K_L)$  comes from a single measurement performed more than 30 years ago [1] and its error dominates the uncertainty in the partial  $K_L$  decay rates. At DAΦNE the Frascati factory almost monochromatic  $K_L$  mesons are produced with  $p \approx 110$  MeV corresponding to a mean path of 340 cm. The KLOE detector is large enough,  $r = 200$  cm, so that 50% of the  $K_L$  decay inside it. The statistical error on the lifetime depends strongly on the time interval covered in the measurement:

$$\frac{\tau}{\tau_0} = \frac{1}{\mathcal{P}} \frac{1 + e^{3T} + (e^T - e^{2T})(3 + T^2)^{0.5}}{(1 + e^T)^3} \quad (1)$$

where  $T = t_{\text{obs}}$  is the time interval observed, in  $K_L$ -lifetime units. With  $T = 0.4$  and  $N = 9 \cdot 10^6$  we can reach an accuracy of  $0.3\%$ .

We have measured the  $K_L$  lifetime using the decay  $K_L \rightarrow \pi^0 \pi^0 \pi^0$  tagged by  $K_S \rightarrow \pi^+ \pi^-$  events. This choice maximizes the number of usable events and minimizes the disturbance of the  $K_L$  decay on the detection of the tagging  $K_S$  decay and therefore the systematic uncertainty.

## 2 Experimental setup

In DA NE electrons and positrons collide with an angle of  $25 \text{ mrad}$  and a center of mass (CM) energy  $\sqrt{s} = M(\Upsilon)$ .  $\Upsilon$ -mesons are produced with a cross section of  $3 \text{ nb}$  and a transverse momentum of  $12.5 \text{ MeV}/c$  toward the center of the collider rings. The energy  $\sqrt{s}$ , the position of the beam crossing point  $(x; y; z)$  and the momentum are determined from Bhabha scattering events. In a typical run of integrated luminosity  $\int L dt = 100 \text{ nb}^{-1}$ , lasting about 30 minutes, the corresponding errors are:  $\sqrt{s} = 40 \text{ keV}$ ,  $p_T = 30 \text{ keV}/c$ ,  $x = 30 \text{ }\mu\text{m}$ , and  $y = 30 \text{ }\mu\text{m}$ .

The detector consists of a large cylindrical drift chamber, DC [2], whose axis, defined as the  $z$ -axis, coincides with the bisectrix of the two beams. The DC is surrounded by a lead-scintillating fiber sampling calorimeter, EMC [3]. DC and EMC are immersed in a solenoidal magnetic field of  $0.52 \text{ T}$  with the axis parallel to the beam's bisectrix. The DC tracking volume extends from  $28.5$  to  $190.5 \text{ cm}$  in radius and is  $340 \text{ cm}$  long. The transverse momentum resolution is  $\frac{\Delta p_T}{p_T} = 0.4\%$ . Vertices are reconstructed with a resolution of  $3 \text{ mm}$ . The calorimeter is divided into a barrel and two endcaps and covers  $98\%$  of the solid angle. Photon energies and arrival times are measured with resolutions  $\frac{\Delta E}{E} = 0.57\% = E \text{ (GeV)}$  and  $\Delta t = 54 \text{ ps} = E \text{ (GeV)}$  50 ps respectively.

Photon entry points are determined with an accuracy  $\Delta z = 1 \text{ cm} = E \text{ (GeV)}$  along the fibers and  $\Delta r = 1 \text{ cm}$  in the transverse direction. A photon is defined as an EMC cluster of energy deposits not associated to a track. We require that the distance between the cluster centroid and the entry point of the nearest extrapolated track be greater than  $3 \text{ }\mu\text{m}$ ,  $\Delta r = \Delta z = \Delta r$ .

The trigger [4] uses information from calorimeter and chamber. The EMC trigger requires two local energy deposits above threshold ( $E > 50 \text{ MeV}$  in the barrel,  $E > 150 \text{ MeV}$  in the endcaps). Rejection of cosmic-ray events is also performed at trigger level, checking for the presence of two energy deposits above  $30 \text{ MeV}$  in the outermost calorimeter planes. The DC trigger is based on the multiplicity and topology of the hits in the drift cells. The trigger has a large time spread with respect to the beam crossing time. It is therefore re-synchronized with the machine radio frequency divided by four,  $T_{\text{sync}} = 10.85$

ns, with an accuracy of 50 ps. During the 2001-2002 data taking the bunch crossing period at DA NE was  $T = 5.43$  ns. The correct collision time,  $T_0$ , of the event is determined on-line during event reconstruction [5].

### 3 Data analysis

$\eta$  mesons decay into  $K_S - K_L$  pairs 34% of the time. Production of a  $K_L$  is tagged by the observation of  $K_S \rightarrow \pi^+ \pi^-$  decay. The  $K_L \rightarrow \pi^0 \pi^0$  decay vertex is reconstructed along the direction opposite to that of the  $K_S$  in the rest frame. The chamber alone measures the  $K_S \rightarrow \pi^+ \pi^-$  decay and therefore the direction of the  $K_L$ . The  $K_L$  decay vertex and the photon energies are obtained from the EMC informations. The data sample, collected during 2001 and 2002, corresponds to an integrated luminosity of  $400 \text{ pb}^{-1}$ . Some  $1.2 \cdot 10^9$   $\eta$  mesons were produced. Additional details can be found in reference [6].  $K_S \rightarrow \pi^+ \pi^-$  decay events must satisfy the following requirements:

- (1) Two tracks with opposite charge, forming a vertex  $V$  in a cylinder with  $r_V < 10 \text{ cm}$ ,  $|z_V| < 20 \text{ cm}$ . No other tracks should be connected to the vertex.
- (2) The  $K_S$  momentum in the rest system, satisfies  $100 < p_{K_S} < 120 \text{ MeV}$ . The  $\pi^+ \pi^-$  invariant mass  $M(\pi^+ \pi^-)$  satisfies  $492 < M(\pi^+ \pi^-) < 503 \text{ MeV}$ .

The efficiency for finding  $K_S \rightarrow \pi^+ \pi^-$  events is 68%. The position of the production point,  $x$ , is determined as the point of closest approach of the  $K_S$  momentum, propagated backwards from the  $K_S$  vertex, to the beam line. The  $K_S \rightarrow \pi^+ \pi^-$  decay provides an almost unbiased tag for the  $K_L$  when it decays into neutral particles and a good measurement of the  $K_L$  momentum,  $p_{K_L} = p_{\pi^+} + p_{\pi^-}$ . The accuracy in the determination of the  $K_L$  direction is obtained from  $K_L \rightarrow \pi^+ \pi^0$  events, measuring the angle between  $p_{K_L}$  and the line joining the production point and the  $\pi^+ \pi^0$  decay vertex. We find  $\sigma_{\theta} = 1.5^\circ$ ,  $\sigma_{\phi} = 1.8^\circ$ .

The position of the  $K_L$  vertex for  $K_L \rightarrow \pi^0 \pi^0$  decays is obtained from the photon arrival times at the EMC. Each photon defines a triangle CDE, see figure 1 (left) where  $l$  is the  $K_L$  path length,  $l$  is the distance from the  $K_L$  decay point D to the entry point E and  $d$  the distance from the cluster to the collision point C. From the known positions of C and E, the  $\angle CED = \theta$  angle and the time spent by the kaon and the photon to cover the path CDE we find the length of CD. There are two solutions, one with D along the  $K_S$  path which is rejected. The position D of the  $K_L$  decay vertex  $\vec{x}_D$  is obtained from the energy weighted average of the two closest  $k_{j,i}$ ,  $k = \pi^0$ ,  $i = 1, 2$ ,  $\vec{x}_D = \frac{\sum_i E_i \vec{x}_{k,i}}{\sum_i E_i}$  where  $i$  is the photon index. Finally we require at least one third photon with  $|k_{j,3} - k_{j,2}| < 5^\circ$  ( $k$ ).

The resolution  $\sigma(l_K)$ , is determined from  $K_L \rightarrow \pi^+ \pi^0$  events comparing  $l_K(\pi^0)$  and  $l_K(\pi^+)$  where the former is the weighted average obtained from the two photons from  $\pi^0$  and  $l_K(\pi^+)$  is the distance between the vertex of the two charged decay pions and the production point. We find  $\sigma(l_K) = 1.66 + 0.57 \cdot 10^{-2} \cdot l_K + 0.45 \cdot 10^{-4} \cdot l_K^2$  cm. The accuracy of the

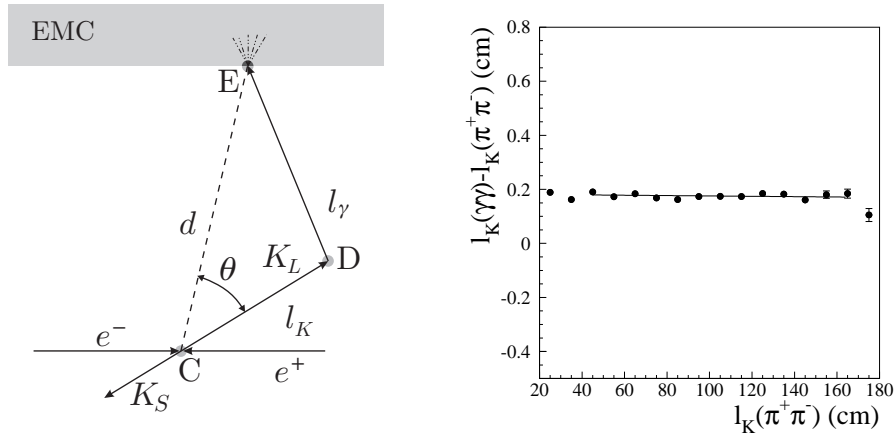


Fig. 1. Left. The CDE triangle. Right. Distribution of the difference  $l_K(\pi^+ \pi^-) - l_K(\pi^+ \pi^0)$  for  $K_L \rightarrow \pi^+ \pi^0$  events as a function of  $l_K(\pi^+ \pi^-)$ . See text.

$l_K$  determination is checked by comparing the  $K_L$  path measured by timing with the calorimeter and, with a much better accuracy, by tracking with the DC, for  $K_L \rightarrow \pi^+ \pi^0$  decays. The path length from the calorimeter timing has on average a constant offset of 2 mm with respect to the value obtained with the DC, figure 1, right. The determination of  $l_K$  depends crucially on the correct identification of the collision time  $T_0$ . Using again  $K_L \rightarrow \pi^+ \pi^0$  events we have verified that  $T_0$  is incorrect less than 0.1% of the time.

The tagging efficiency has been evaluated by MC as a function of  $l_K$  for the dominant  $K_L$  decay channels. The results are shown in Fig. 2. The difference in

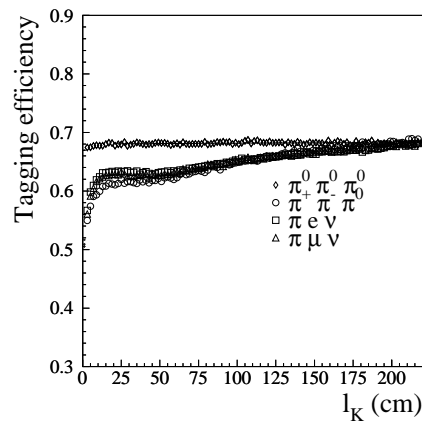


Fig. 2. Tagging efficiency as a function of  $l_K$  for the main  $K_L$  decay modes.

tagging efficiency among the  $K_L$  decay modes is mainly due to the dependence of the trigger efficiency. Only the calorimeter trigger [4], is used for the present analysis. The trigger efficiency is, on average, 100% for  $K_L \rightarrow 0^+ 0^+ 0^+$  and between 85–95% for charged  $K_L$  decays. The trigger efficiency also depends on the position on the  $K_L$  decay vertex. Another contribution is the dependence of the reconstruction efficiency for the pion tracks from  $K_S \rightarrow \pi^+ \pi^-$  on the presence of other tracks in the drift chamber. This contribution depends on the position of the  $K_L$  decay point and affects mainly events with  $K_L \rightarrow$  charged particles near to the production point.

The tagging efficiency for the  $K_L \rightarrow 0^+ 0^+ 0^+$  channel has a small linear dependence with  $l_k$ , with a slope of  $b = (1.2 \pm 0.2) \cdot 10^{-5} / \text{cm}$ , and a constant  $a = (68.04 \pm 0.01)\%$ .

#### 4 $K_L \rightarrow 0^+ 0^+ 0^+$ acceptance

The  $K_L \rightarrow 0^+ 0^+ 0^+$  decay has a relatively large BR, 21%, and has very low background.  $K_L \rightarrow 0^+ 0^+ 0^+$  events are accepted if at least three calorimeter clusters are found satisfying:

- (1) Energy larger than 20 MeV.
- (2) Distance from any other cluster larger than 50 cm.
- (3) No association to a chamber track.
- (4)  $\sum_{k_{ji}} l_{k_j} < 5 \cdot \langle l_k \rangle$ , where  $l_k$  is the energy weighted average of the closest two  $l_{k_{ji}}$ .

For the  $K_L$  lifetime measurement, we retain events with  $40 < l_k < 165$  cm and a polar angle in the interval  $40^\circ < \theta < 140^\circ$ . These two conditions define the fiducial volume (FV). Main sources of event losses are: 1) geometrical acceptance; 2) cluster energy threshold; 3) merging of clusters; 4) accidental association to a charged track; 5) Dalitz decay of one or more  $0^+$ 's. The effect of these inefficiencies is to modify the relative population for events with 3, 4, 5, 6, 7 and 8, clusters with a loss of global efficiency of 0.8%.

Monte Carlo (MC) simulations, based on the KLOE standard MC [5] show that event acceptance with the above selection has a linear dependence on  $l_k$ ,  $\langle \epsilon \rangle = (0.9921 \pm 0.002) + (1.9 \pm 0.2) \cdot 10^{-5} \cdot l_k$  with  $l_k$  in cm, (figure 3, left) mainly due to the vertex reconstruction efficiency. This has also been checked using  $K_L \rightarrow \pi^+ \pi^- 0^+$  events both from data and MC. We find the same linear dependence, with compatible slopes within their statistical uncertainties, figure 3, right.

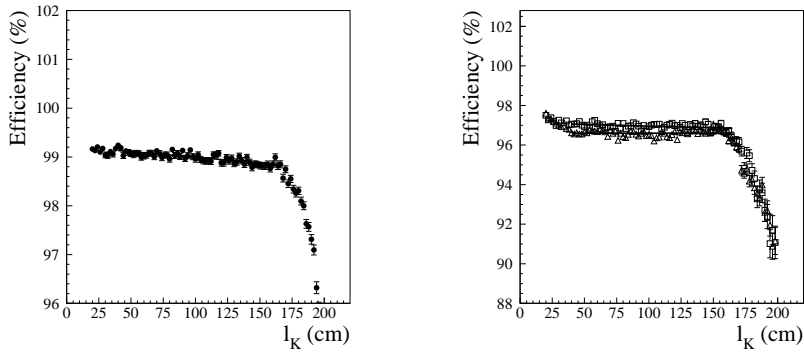


Fig. 3. Left: Vertex reconstruction efficiency as a function of the decay path length for  $K_L \rightarrow \pi^0 \pi^0 \pi^0$  Monte Carlo events. Right: the same for  $K_L \rightarrow \pi^+ \pi^0$  data (dots) and Monte Carlo (squares) events.

A comparison between data and MC of photon multiplicity and total energy distribution for  $K_L \rightarrow \pi^0 \pi^0 \pi^0$  decays shows that only events with 3 and 4 clusters contain some background. Background, mostly to the three cluster events, is due to  $K_L \rightarrow \pi^+ \pi^0$  decays where one or two charged pions produce a cluster not associated to a track and neither track is associated to the  $K_L$  vertex. Other sources of background are  $K_L \rightarrow \pi^0 \pi^0$  decays (possibly in coincidence with machine background showering close to the collision point generating soft neutral particles) and  $K_S \rightarrow \pi^0 \pi^0$  following the  $K_L \rightarrow K_S$  regeneration in the DC material. The  $K_L \rightarrow \pi^+ \pi^0$  background and the other ones are strongly reduced by requiring at least one cluster in the barrel with  $E > 50$  MeV and no tracks approaching the  $K_L$  line of sight by less than 20 cm. The efficiency vs  $l_K$  has been found by MC. It is almost flat with an average 55% inside the FV.

In Table 1 we show the fractions of the background components before and after the background cuts. The background contamination is reduced from 4.9% to 1.3% with an efficiency on the signal of 99.6%. The distributions of the total photon energy for events with 3;4;5;6;7; 8 photons are shown in Fig. 4. For three and four photons event samples the different contributions from the residual background components are also shown.

The fractions of events with  $N = 3;4;5;6;7; 8$  in the FV are given in Table 2, together with MC results. The few percent differences between data and MC are mostly due to a higher amount of split clusters in the MC than in the data.

K <sub>L</sub> channel	N = 3 before cuts		N = 3 after cuts	
	Events	B / (S + B)	Events	B / (S + B)
signal+ backgrounds	10,536,674		10,114,899	
all backgrounds	518,520	4.92 %	133,535	1.32 %
K <sub>L</sub> ! + 0	325,076	3.08 %	44,917	0.44 %
K <sub>L</sub> !	28,917	0.28 %	3,583	0.03 %
K <sub>L</sub> ! e	49,140	0.47 %	6,062	0.06 %
K <sub>L</sub> ! 0 0	43,436	0.41 %	42,313	0.42 %
K <sub>L</sub> ! K <sub>S</sub> ! 0 0	30,273	0.29 %	28,166	0.28 %
K <sub>L</sub> ! other	41,298	0.39 %	8440	0.08 %

Table 1

Event types in the fiducial volume from Monte Carlo before and after background cuts. The background contamination  $B = (S + B)$  is also shown.

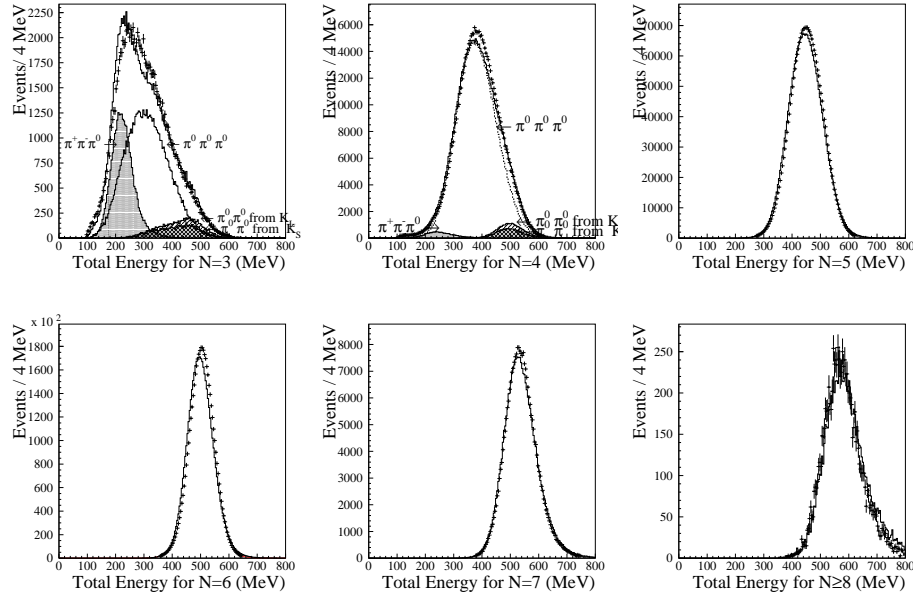


Fig. 4.  $K_L \rightarrow 0 0 0$  selection: distribution of the total energy for events with 3, 4, 5, 6, 7 and 8 photon clusters. Dots are data, solid histogram is Monte Carlo simulation for  $K_L \rightarrow$  all channels. Monte Carlo histograms are normalized to the same number of entries of Data.

## 5 Fit of the proper time distribution

The  $K_L$  proper time,  $t$ , is obtained event by event dividing the decay length  $l_K$  by  $\beta\gamma$  of the  $K_L$  in the laboratory,  $t = l_K / (\beta\gamma c)$ . In figure 5 we show the  $t$  distribution obtained with  $14.7 \cdot 10^6$  tagged  $K_L \rightarrow 0 0 0$  events. The residual 1.3% background is subtracted using MC results. The variation of the vertex reconstruction efficiency as a function of the decay length is taken into account by correcting bin by bin in the  $t$  distribution with the MC

Number of clusters	Data		Monte Carlo	
3	1.163	0.004 %	0.980	0.003 %
4	7.64	0.01 %	7.01	0.01 %
5	30.22	0.02 %	28.65	0.02 %
6	57.77	0.03 %	60.12	0.03 %
7	3.091	0.006 %	3.074	0.001 %
8	0.106	0.001 %	0.151	0.001 %

Table 2

Fraction of events with 3,4,5,6,7 and 8 neutral clusters connected to the  $K_L$  decay vertex in data and Monte Carlo.

$K_L \rightarrow 3^0$  efficiency (figure 3, left) and the data/MC efficiency ratios for  $K_L \rightarrow 3^0$  (figure 3, right). The statistical uncertainty of the efficiency ( $\pm 0.1\%$ ) estimate is included in the error.

The  $t$  distribution is fitted with an exponential function over the range  $6 < t < 24.8$  ns. This corresponds to a time interval  $T = t = 0.37$ . With  $8.5 \cdot 10^6$  events in the  $t$  region we obtain:

$$\tau = (50.87 \pm 0.17) \text{ ns}$$

with a  $\chi^2$ -value of 58 for 62 degrees of freedom (see Fig. 5).

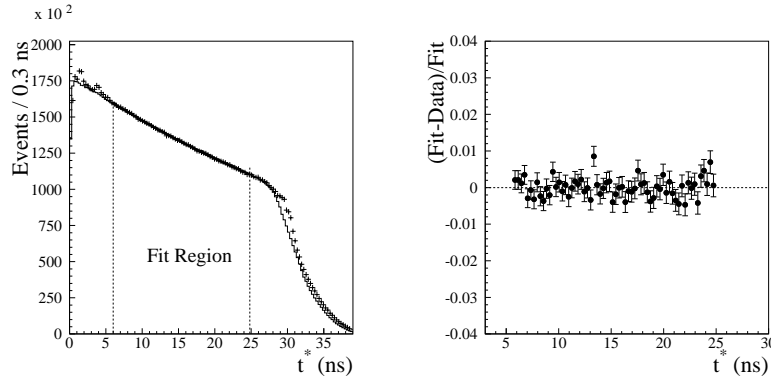


Fig. 5. Fit of the proper time distribution (left) and residuals of the  $t$  (right). Crosses are data and solid histogram is Monte Carlo. The fit is shown as the thick solid line.

## 6 Systematic uncertainties

The number of  $K_L \rightarrow 3^0$  at the end of the selection is given by:

$$N_{3^0}(k) = N_{3^0}(0) \sum_{\text{tot}} \binom{0}{k} e^{-1} = e^{-1} \sum_{\text{tot}} \binom{0}{k} e^{-(1-k)^2} = 2^{-2} \binom{0}{k} d_{k^0} + N_{\text{bck}}(k); \quad (2)$$

where  $N_{\text{bck}}$  is the residual background at the end of the signal selection,  $\epsilon_{\text{tot}}(l_K^0)$  is the signal efficiency ( $\epsilon_{\text{tot}} = \epsilon_{\text{tag}} \epsilon_{\text{sel}}$ ),  $e^{-(l_K - l_K^0)^2 / 2 \sigma_K^2}$  is the vertex resolution function. Finally  $\tau_E = (1 - \epsilon_L + \epsilon_I)^{-1}$ , is the effective mean decay length taking into account the  $K_L$  interactions inside the chamber (in the gas mixture and wires) and  $\tau_L$  is the mean  $K_L$  decay length.

Many effects distort the proper time distribution and have been corrected for. The uncertainty in the corrections is properly included in the systematic error on the  $K_L$  lifetime. The tagging efficiency has a linear dependence on  $k_T$  with a constant term  $a = (0.6804 \pm 0.0003)$  and a slope  $b = (1.2 \pm 0.2) \cdot 10^{-5} / \text{cm}$ . It results in a correction of 0.6% with a systematic uncertainty of 0.1%. We also vary the threshold of the cluster energy of the pions from  $K_S$  from 40 to 70 MeV in 10 MeV steps. The slope changes by 0.5% with a systematic uncertainty of 0.25%. As discussed, the efficiency has been corrected for its dependence on  $k_T$ . We assign a systematic error of 0.2% due to the statistical uncertainty on the slope of the data/Monte Carlo efficiency ratios evaluated with  $K_L \rightarrow \pi^+ \pi^0$  events. We investigate the effects of the cluster energy threshold for photons  $E_{\text{thr}}$ , by varying  $E_{\text{thr}}$  from 10 to 35 MeV in steps of 5 MeV and repeating the full analysis. The  $\tau$  changes by 0.2% for  $15 < E_{\text{thr}} < 35$  MeV which we take as a systematic uncertainty. The total systematic uncertainty due to the event selection is therefore 0.3%. Finally the effect of the vertex resolution on the  $\tau$  result is below 0.1%, which we neglect.

The background (table 1) is subtracted from the proper time distribution using MC simulation. An additional systematic error is due to uncertainties in background scale and  $k_T$  shape in the three and four event samples. Comparing bin by bin data and MC distributions, we find agreement at the 10% level with a small linear dependence on  $k_T$ . Changing the background scale changes the  $\tau$  result by 0.2%. Correction for the background slope changes the  $\tau$  result by +0.15% with an uncertainty of 0.06% due to the statistical fluctuation in the slope value.

$K_L$  interactions with the material inside the chamber bias the lifetime measurement since they reduce the  $K_L$  mean path by  $(1 - \epsilon_L - \epsilon_I)$  [6]. The interaction rates for regeneration and  $\pi^0$  production are determined from data [7]. The contribution of the regeneration in the DC material is found to be 3 times lower in data than the MC prediction. In the data the contribution of the total nuclear interactions is 0.33% to which we assign a conservative error of 50%,  $(0.33 \pm 0.16)\%$ . Therefore, the  $K_L$  lifetime is corrected by +0.33% with a systematic uncertainty of 0.16%. Uncertainties in the DC momentum scale and the absolute EMC time scale enter directly in the proper time evaluation  $t = k_T / (\beta c)$  and give systematic errors respectively of 0.1% [5] and  $7 \cdot 10^{-4}$  (figure 1, right).

The  $\tau$  stability has been checked by changing the lower limit of the time interval used in the fit between 6 ns and 12 ns and the upper between 21 ns and 28 ns, independently. No change in  $\tau_L$  is found within its statistical error. We have also checked the  $\tau$  stability vs polar angle dividing the fiducial volume in two regions containing the same number of events. Specially we chose events with  $0.342 < |\cos \theta| < 0.766$  and  $|\cos \theta| < 0.342$ . The values of  $\tau_L$  from the two zones are statistically well consistent.

In table 3 we summarize the corrections to be applied to the lifetime  $\tau$  result and the corresponding systematic uncertainties.

source	correction	systematic uncertainty
tagging efficiency	0.6%	0.25%
acceptance	bin by bin	0.3%
selection efficiency	bin by bin	$5 \cdot 10^5$
vertex resolution	-	0.1%
background subtraction	bin by bin, + 0.2%	0.2%
background shape	+ 0.15%	0.06%
nuclear interactions	+ 0.33%	0.16%
momentum scale	-	0.1%
time scale	-	0.07%
total	+ 0.1%	0.49%

Table 3

Summary of corrections and systematic uncertainties.

The corrections add to + 0.1% and the central value of the  $\tau$  is moved accordingly. The systematic error of 0.49% is at present dominated by the uncertainty on the dependence of tagging efficiency with  $|\cos \theta|$  and by background subtraction. The final result is:

$$\tau_L = (50.92 \pm 0.17_{\text{stat}} \pm 0.25_{\text{syst}}) \text{ ns} = (50.92 \pm 0.30) \text{ ns}$$

This result differs by 1.2 from the other direct measurement  $\tau_{K_L} = (51.54 \pm 0.44) \text{ ns}$  [1] and by 1.8 from the PDG 2004 fit [8],  $\tau_{K_L} = (51.8 \pm 0.4) \text{ ns}$ .

#### Acknowledgements

We thank the DAFNE team for their efforts in maintaining low background running conditions and their collaboration during all data-taking. We want to thank our technical staff: G.F. Fortugno for his dedicated work to ensure an efficient operation of the KLOE Computing Center; M. Anelli for his continuous support to the gas system and the safety of the detector; A. Balla, M. Gatta, G. Corradi and G. Papalino for the maintenance of the electronics;

M. Santoni, G. Paoluzzi and R. Rosellini for the general support to the detector; C. Piscitelli for his help during major maintenance periods. This work was supported in part by DOE grant DE-FG-02-97ER41027; by EURODAPHNE, contract FMRX-CT98-0169; by the German Federal Ministry of Education and Research (BMBF) contract 06-KA-957; by Graduiertenkolleg H.E. Phys. and Part. Astrophys. of Deutsche Forschungsgemeinschaft, Contract No. GK 742; by INTAS, contracts 96-624, 99-37; and by the EU Integrated Infrastructure Initiative Hadron Physics Project under contract number RII3-CT-2004-506078.

## References

- [1] K. G. Vosburgh et al., Phys. Rev. Lett. 26 (1971), 866 and Phys. Rev. D 6 (1972), 1834.
- [2] The KLOE Collaboration, M. Adinolfi et al., Nucl. Instr. and Meth. A 488 (2002) 51.
- [3] The KLOE Collaboration, M. Adinolfi et al., Nucl. Instr. and Meth. A 482 (2002) 363.
- [4] The KLOE Collaboration, M. Adinolfi et al., Nucl. Instr. and Meth. A 492 (2002) 134.
- [5] A. Ambrosino et al., Nucl. Instr. Meth. A 534 (2004), 403.
- [6] G. Lanfranchi Direct measurement of the  $K_L$  lifetime, KLOE note n. 203, July 2005. URL: <http://www.infn.it/kloe/pub/knote/kn203.ps>
- [7] M. Antonelli, P. Beltrame, M. Dreucci, M. Moulson, M. Palutan, A. Sibidanov, Measurements of the absolute branching fractions for the dominant  $K_L$  decays, the  $K_L$  lifetime and  $\beta_{us}^j$  with the KLOE detector, KLOE note n. 204 (2005). URL: <http://www.infn.it/kloe/pub/knote/kn204.ps>
- [8] S. Eidelman et al., Phys. Lett. B 592 (2004) 1